Received: 30 September 2019 | Revised: 4 February 2020 | Accepted: 5 February 2020

DOI: 10.1111/bcp.14256

ORIGINAL ARTICLE

A semi-mechanistic model based on glutathione depletion to describe intra-individual reduction in busulfan clearance

Jurgen B. Langenhorst[1,2] | Jill Boss[3] | Charlotte van Kesteren[4] | Arief Lalmohamed[5] | Jürgen Kuball[1,6] | Antoine C. G. Egberts[5,7] | Jaap Jan Boelens[8] | Alwin D. R. Huitema[5,9] | Erik M. van Maarseveen[5]

[1]Laboratory of Translational Immunology, University Medical Centre Utrecht, Utrecht University, Utrecht, The Netherlands

[2]Model-informed Drug Development Consultant, Pharmetheus AB, Uppsala, Sweden

[3]Hospital Pharmacy, St Jansdal Hospital, Harderwijk, The Netherlands

[4]Hospital Pharmacy, Albert Schweitzer Hospital, Dordrecht, The Netherlands

[5]Department of Clinical Pharmacy, University Medical Centre Utrecht, Utrecht University, Utrecht, The Netherlands

[6]Department of Hematology, University Medical Centre Utrecht, Utrecht University, Utrecht, The Netherlands

[7]Department of Pharmacoepidemiology & Clinical Pharmacology, Faculty of Science, Utrecht University, Utrecht, The Netherlands

[8]Stem Cell Transplant and Cellular Therapies; Pediatrics, Memorial Sloan Kettering Cancer Centre, New York City, New York, USA

[9]Department of Pharmacy & Pharmacology, Netherlands Cancer Institute, Amsterdam, The Netherlands

Correspondence
Erik van Maarseveen, Department of Clinical Pharmacy, University Medical Centre Utrecht, Utrecht, Utrecht University, Heidelberglaan 100: D.00.X, 3584 CX, Utrecht, The Netherlands.
Email: e.m.vanmaarseveen@umcutrecht.nl

Funding information
Stichting Kinderen Kankervrij, Grant/Award Number: 190

Aim: To develop a semi-mechanistic model, based on glutathione depletion and predict a previously identified intra-individual reduction in busulfan clearance to aid in more precise dosing.

Methods: Busulfan concentration data, measured as part of regular care for allogeneic hematopoietic cell transplantation (HCT) patients, were used to develop a semi-mechanistic model and compare it to a previously developed empirical model. The latter included an empirically estimated time effect, where the semi-mechanistic model included theoretical glutathione depletion. As older age has been related to lower glutathione levels, this was tested as a covariate in the semi-mechanistic model. Lastly, a therapeutic drug monitoring (TDM) simulation was performed comparing the two models in target attainment.

Results: In both models, a similar clearance decrease of 7% (range −82% to 44%), with a proportionality to busulfan metabolism, was found. After 40 years of age, the time effect increased with 4% per year of age (0.6–8%, $P = 0.009$), causing the effect to increase more than a 2-fold over the observed age-range (0–73 years). Compared to the empirical model, the final semi-mechanistic model increased target attainment from 74% to 76%, mainly through better predictions for adult patients.

Conclusion: These results suggest that the time-dependent decrease in busulfan clearance may be related to gluthathione depletion. This effect increased with older age (>40 years) and was proportional to busulfan metabolism. The newly constructed semi-mechanistic model could be used to further improve TDM-guided exposure target attainment of busulfan in patients undergoing HCT.

KEYWORDS

chemotherapy – oncology, drug safety – clinical pharmacology, pharmacokinetics, therapeutic drug monitoring – clinical pharmacology

The authors confirm that the Principal Investigator for this paper is Dr E. M. van Maarseveen and that he had direct clinical responsibility for patients.

1 | INTRODUCTION

Allogeneic hematopoietic cell transplantation (HCT) is a high-risk, but potentially curative treatment for a variety of malignant and non-malignant haematological disorders. Unfortunately, treatment-related mortality is substantial (10–40%), implying an urgent need of further optimization of this procedure.[1]

Prior to HCT, the bone marrow and immune system of the host are ablated by means of a preparative conditioning regimen. In these conditioning regimens, busulfan is the most frequently used drug.[2] Busulfan is usually administered over a 4-day period and has a narrow therapeutic window, where an exposure corresponding with an area under the plasma concentration–time curve (AUC) from the first dose until infinity ($AUC_{t0-\infty}$) of 80 – 100 mg*h/L (≈20000–25000 μMol*min) has been associated with optimal treatment outcomes in a myeloablative setting.[3–5] Lower exposures have been associated with more frequent relapse or graft failure, and higher exposures with increased probability of severe toxicity and treatment-related mortality.

Therapeutic drug monitoring (TDM)-guided dosing is recommended to better attain this narrow target exposure.[6] Indeed, the use of TDM has been proven to increase overall survival by 20% compared to fixed dosing in a randomized controlled trial setting.[7] However, the attainment of the desired busulfan target exposure is still challenging due to an intra-individually variable clearance reduction from day 1 to day 4 with associated variability of 11–15%, as has previously been shown.[8–10] These effects respectively limit the accuracy and precision of TDM based on samples measured at the first day of conditioning. As the mechanism behind this time-dependent decrease is unknown, the effect has been implemented empirically, where a more mechanistic approach may better predict inter-individual differences in clearance reduction.

The primary route of busulfan clearance is through extensive metabolism in the liver: only 2% of busulfan is excreted unchanged in urine. Initial inactivation occurs by conjugation to glutathione (GSH), both spontaneously and aided by an enzyme.[11,12] The busulfan–GSH conjugate is further metabolized via two parallel routes: β-elimination, catalysed by cystathionine γ-lyase, forming tetrahydrothiophene, pyruvate and ammonium; or through conversion to an *N*-acetylated cysteine conjugate by *N*-acetyltransferase. Polymorphisms of the enzyme glutathione-*S*-transferase (GST) have been used to better predict busulfan clearance a priori,[13–18] but such predictions are obviated by the use of TDM. Interestingly, it has also been shown that in patients treated with high-dose busulfan, levels of the substrate GSH decrease by approximately 75%.[19] In addition, higher baseline GSH concentrations were correlated with an up to 2-fold increased busulfan clearance.[19] Therefore, we hypothesize that busulfan-mediated GSH depletion causes the observed reduction in clearance. Because of the lack of GSH concentration–time data, a fully mechanistic approach to test this hypothesis was not possible. Nevertheless, patients with a high initial busulfan clearance may exhibit a higher decrease in clearance, following from more pronounced GSH depletion. This hypothesis was explored in a semi-mechanistic population pharmacokinetic model, ultimately aiming to achieve more predictable busulfan exposure and thus more predictable outcomes.

What is already known about this subject

- Busulfan has a narrow therapeutic window, necessitating precise exposure-guided dosing.
- Within-patient busulfan clearance varies over time, compromising the efficacy of pharmacokinetic-guided dose adjustments.

What this study adds

- Intra-individual decrease of busulfan clearance is proportional to busulfan metabolism.
- Older age (>40 years) is associated with a stronger time-dependent decrease.
- Therapeutic drug monitoring can be further improved by using a newly developed semi-mechanistic model implementing the aforementioned effects.

2 | METHODS

2.1 | Patients

Included patients were those who received (non)myeloablative conditioning before HCT between September 2005 and January 2017 at the University Medical Centre (UMC) Utrecht and for whom plasma concentration data were available. Data consisted of plasma concentrations measured as part of regular care for HCT patients. The dataset then contained all UMC patients included for the previously developed empirical model,[8] which contained data up to 2008, plus all adult patients and children transplanted after September 2009. Patients were included after written informed consent was acquired. Ethical approval by the institutional medical ethics committee of the UMC Utrecht was obtained under protocol number 11/063.

2.2 | Procedures

The conditioning regimen consisted of intravenous busulfan combined with either fludarabine (+/− clofarabine) or cyclophosphamide. In selected patients transplanted before 2011, targeted busulfan was combined with cyclophosphamide at a cumulative dose of 120 or 200 mg/kg. Four days of busulfan were followed by 2 days (120 mg/m^2) or 4 days (200 mg/m^2) of

cyclophosphamide, starting on days −7 and −9, respectively. Busulfan and fludarabine conditioning was administered on days −5 to −2 relative to HCT and consisted of a 1-hour-infusion of fludarabine-phosphate (40 mg/m^2) directly followed by a 3-hour infusion of busulfan (Busilvex, Pierre Fabre: Castres, France). A 1-hour infusion of clofarabine (30 mg/m^2) preceded a reduced dose of fludarabine (10 mg/m^2) in children with haematological malignancies. Rabbit antithymocyte globulin (rATG) was added in the unrelated donor HCT setting: 4-hour infusions on 4 consecutive days from day −9 (10 mg/kg < 30 kg, 7.5 mg/kg > 30 kg) for children and 12-hour infusions on 4 consecutive days from day −12 (6 mg/kg) for adults. To patients receiving rATG, clemastine (0.03 mg/kg up to 2 mg), paracetamol (60 mg/kg up to 4 g) and 2 mg/kg prednisolone with a maximum of 100 mg were given intravenously prior to rATG infusion. *N*-acetylcysteine was not routinely administered during conditioning.

Busulfan was targeted using a dosing algorithm[8] and TDM to a myeloablative cumulative 4-day exposure of 90 mg*h/L ≈ 22000 μMol*min (current target), 80 mg*h/L ≈ 20000 μMol*min (target before 2011), 60 mg*h/L ≈ 15000 μMol*min (reduced intensity) or 30 mg*h/L ≈ 7300 μMol*min for Fanconi anaemia patients (expressed as the area under the curve for all doses [$AUC_{T0} - \infty$]). According to the busulfan TDM protocol, plasma samples were drawn on the first and/or second day of conditioning. In the case of large dose adjustments (>50%), samples were also drawn on subsequent days for confirmatory reasons. Additional samples were taken for all patients at day 4 of conditioning to evaluate target exposure attainment. In general, plasma samples were taken at 5 minutes and 1, 2 and 3 hours after the end of busulfan infusion. For a subset of patients, additional samples were collected from 4 to 20 hours post infusion. Samples were analysed with a validated liquid chromatography mass spectrometry (LC–MS) method according to Langman et al.[20] In children treated before September 2008 a previously published high-performance liquid chromatography-ultraviolet (HPLC–UV) method was used.[21,22] For dose adjustment, the individual clearance was estimated with a Bayesian approach using the individual samples and a one-compartmental pharmacokinetic analysis in the software package of MwPharm.[23] The individual clearance was estimated and the doses for the subsequent days were calculated using equation (1).

$$\text{dose}_{\text{adjusted}} = \left(\text{target}(\text{AUC}_{t_0-\infty}) - \frac{\text{dose}_{\text{administered}}}{\text{CL}_{\text{estimated}}}\right) \times \text{CL}_{\text{estimated}} \quad (1)$$

2.3 | Pharmacokinetic model design and evaluation

The previously published model by Bartelink et al. was used as the basis for a structural model.[8] In that model, weight was included as a covariate on clearance and volume of distribution of the central compartment (V_1). Clearance was included using an empirical weight-changing allometric exponent (equation (2)) and V_1 was described by a constant empirically estimated exponent. A stepwise effect of time on clearance was estimated using separate values for day = 1 and day > 1. No further covariates were included.

$$\text{CL}_i = \text{CL}_{43\text{kg}} \times \frac{\text{BW}_i^{\text{I} \times \text{BW}_i^{\text{P}}}}{43\,\text{kg}} \quad (2)$$

In addition to this model, henceforth referred to as the empirical model, allometric scaling to weight was added for volume of distribution of the peripheral compartment (V_2) and inter-compartmental clearance between V_1 and V_2 ($_Q$), using fixed exponents of 1 and 0.75, respectively. Next, the stochastic model was optimized with a higher number of subjects. Inter-individual variability (IIV) and correlations between IIV were tested for clearance, V_1, V_2, and Q. Inter-occasion variability (IOV) was tested only on V_1 and clearance to preserve parsimony. Both IIV and IOV were assumed to be log-normally distributed. The proportional residual variability from the original model was retained, but variances were estimated for the different methods of quantification (HPLC–UV and LC–MS) differed.

For the semi-mechanistic model, the above-mentioned expanded empirical model was used as a basis, but without the empirical time effect. A compartment was then added representing the relative amount of GSH available at any time, where the initial amount was assumed to be 1. The model assumed a zero-order synthesis and first-order elimination of GSH. As the relative amount of GSH at baseline is set at 1, the zero-order synthesis rate constant equals the first-order elimination rate constant at equilibrium. Busulfan in the central compartment was assumed to be metabolized in a GSH-dependent way. The full model is depicted in Figure 1 and described in equations (3), (4) and (5).

$$\frac{dA_{\text{bu}_1}}{dt} = -A_{\text{bu}_1} \times \left(k_{\text{bu}_{10}} \times A_{\text{GSH}} + k_{12}\right) + A_{\text{bu}_2} \times k_{\text{bu}_{21}} \quad (3)$$

$$\frac{dA_{\text{bu}_2}}{dt} = A_{\text{bu}_1} \times k_{\text{bu}_{12}} - A_{\text{bu}_2} \times k_{\text{bu}_{21}} \quad (4)$$

$$\frac{dA_{\text{GSH}}}{dt} = \frac{S_{\text{GSH}}}{V_1} \times A_{\text{GSH}} \times k_{10} \times A_{\text{bu}_1} - k_{\text{GSH}_{\text{baseline}}} \times A_{\text{GSH}} + k_{\text{GSHsynthesis}} \quad (5)$$

Compartments bu_1 and bu_2 represent the central and peripheral compartments of busulfan, respectively, and GSH represents the theoretical GSH compartment. The elimination and distribution constants for busulfan are depicted by k_{bu}. The first-order elimination constant for GSH is depicted by $k_{\text{GSHbaseline}}$ and the zero-order synthesis constant by $k_{\text{GSHsynthesis}}$. S_{GSH} is a scaling factor between busulfan metabolism and relevant GSH depletion.

As no GSH concentrations were available in the current analysis, busulfan metabolism was used as a surrogate marker and full GSH dynamics could not be reconstructed, therefore the following assumptions were made: (1) the last two terms of equation (5) represent the endogenous GSH turnover and were assumed to sum up to 0 at baseline; (2) when A_{GSH} decreases as a result of busulfan metabolism, the sum of endogenous turnover terms exceeds zero, resulting in net GSH

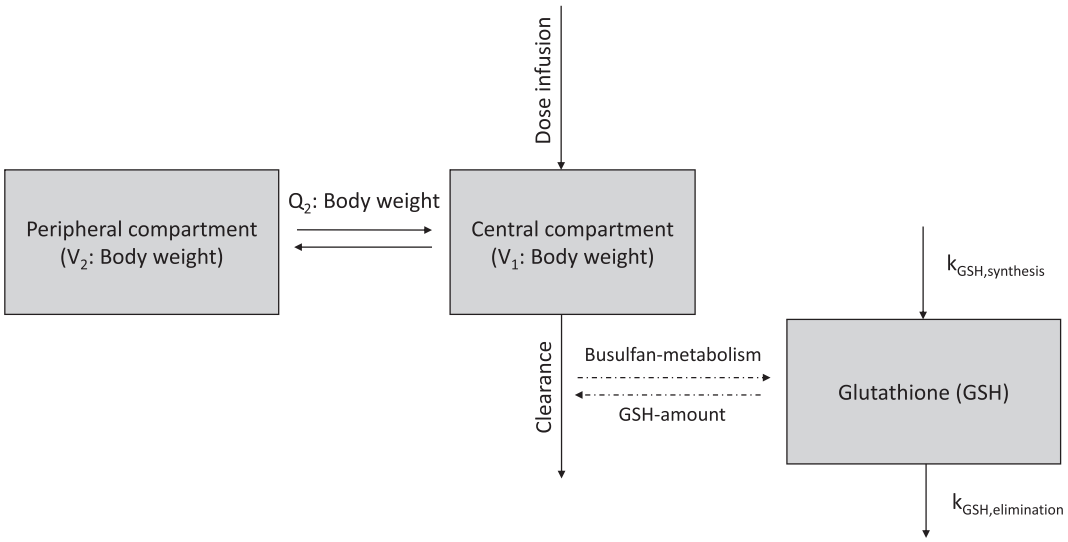

FIGURE 1 Semi-mechanistic busulfan model structure. Busulfan is infused to and eliminated from (clearance) the central compartment (V_1); busulfan distributes reversibly to the peripheral compartment (V_2) with a rate determined by the inter compartmental clearance, Q_2. Glutathione is synthesized and eliminated according to $k_{GSH,synthesis}$ and $A_{GSH} \times k_{GSH,elimination}$, respectively. These terms are assumed to be the same at steady state. The dashed lines indicate the influence busulfan metabolism and glutathione amount have on each other and the solid lines depict transport

production; it was assumed that this net synthesis was negligible compared to busulfan-dependent depletion, thus equation (5) was simplified to equation (6).

$$\frac{dA_{GSH}}{dt} = \frac{S_{GSH}}{V_1} \times A_{GSH} \times k_{10} \times A_{bu_1} \quad (6)$$

The factor S_{GSH} is a scaling factor to associate busulfan metabolism with relevant depletion of GSH. Relevance is defined as depletion to an extent that it becomes a limiting factor in busulfan clearance (as this drives estimation of S_{GSH}). As GSH was set to an absolute amount equal for all individuals (1 at baseline), a scaling factor was necessary for consistent GSH amounts relative to busulfan amounts to account for the highly variable body size and concurrent dosing in the current dataset. Therefore, S_{GSH} was scaled to individual values for V_1, thus assuming the volume of distribution for GSH to be proportional to V_1 of busulfan.

Age has a reported relation to human GSH abundance and turnover,[24,25] and was tested as a continuous covariate on S_{GSH}.

A population approach based on nonlinear mixed-effects modelling was applied[26] using the software package NONMEM (version 7.3.0, Icon, Hanover, MD, USA). Pirana (version 2.9.5) and R (version 3.3.3) were used for workflow management and data handling and visualization, respectively.[27,28] The stochastic approximation and estimation maximization and Monte Carlo importance sampling estimation maximization assisted by mode a posteriori estimation as implemented in NONMEM were used for estimation and objective function calculation, respectively.

The structural and covariate model with corresponding estimates had to be scientifically and biologically plausible. A visual inspection of model performance was done through standard goodness-of-fit plots. Examples of these plots are observed concentrations plotted versus individual and population predicted concentrations, and conditional weighted residuals versus time and observed concentrations.[29] Particular emphasis was given to goodness-of-fit plots stratified for different days (occasions) to assess the time-dependent performance. Hierarchical models were statistically compared after backward deletion of the term or covariate of interest. This comparison was done by the objective function value (OFV) (ΔOFV), which follows a chi-square distribution. A ΔOFV of −3.84 then corresponds to a P value of 0.05 for addition of one parameter (ie 1 degree of freedom).

Several other evaluation techniques were performed, all in accordance with European Medicine Agency and Food and Drug Administration guidelines for population pharmacokinetic analyses.[30,31] A sampling importance resampling (SIR) evaluation (final step: 2000 samples, 1000 resamples) was performed to estimate parameter precision. To assess the simulation properties, prediction-corrected visual predictive checks (VPCs) were created to judge predictive performance of the final model as compared to the observed concentrations. The prediction-corrected VPC allows for variability in dosing.[32] In this analysis, the observed concentration data and its median and 95% confidence interval (CI) were compared to the 95% CI of the predicted mean, 2.5th and 95th percentiles, derived from 1000 model simulations.

2.4 | TDM-guided target attainment evaluation

This analysis aimed to compare the Bayesian forecasting properties of both models in a TDM setting. For this, all patients targeted to an $AUC_{t0} - \infty$ of 90 mg*h/L with samples available on at least

days 1 and 4 were included. TDM was simulated by using both models to predict busulfan clearance throughout conditioning, using only the samples available on day 1. Subsequently, equation (1) was used to calculate the required dose for days 2, 3 and 4. The predicted $AUC_{t0} - \infty$ was calculated by using the post hoc estimates estimated using all available pharmacokinetic data and dosing as calculated from the day 1-TDM simulations. The target $AUC_{t0} - \infty$ attainment rates were assessed for both models.

TABLE 1 Patient characteristics[a]

Weight at HCT (kg)	50 (3.7–130)
Age at HCT (years)	14 (0.16–73)
Age category at HCT	
Children: 0–12 years	159 (41%)
Adolescents: 12–20 years	91 (24%)
Adults: 20–40 years	35 (9%)
Adults: 40–60 years	59 (15%)
Adults: 60+ years	43 (11%)
Samples (no. per patient)	15 (5–24)
Sex	
Male	233 (60%)
Female	154 (40%)
Cell source	
Cord blood	179 (46%)
Peripheral blood stem cells	120 (31%)
Bone marrow	76 (20%)
Autologous	7 (1.8%)
Haplo-cord	5 (1.3%)
Conditioning regimen	
Bu90/flu	215 (56%)
Bu90/Clo/flu	68 (18%)
Bu < 90/cy	46 (12%)
Bu < 90/flu	44 (11%)
Other	14 (3.6%)
Diagnosis	
Leukemia	179 (46%)
Benign[a]	132 (34%)
MDS[c]	33 (8.5%)
Plasma cell disorder[c]	24 (6.2%)
Lymphoma[c]	19 (4.9%)
Serotherapy	
Serotherapy	303 (78%)
No serotherapy	84 (22%)

Abbreviations: BuXX, busulfan targeted to XX mg*h/L; Clo, clofarabine; Flu, fludarabine; HCT, hematopoietic cell transplantation; MDS, myelodysplastic syndrome.
[a]Characteristics are displayed per patient–transplantation combination (one patient was transplanted twice).
[b]Patients transplanted for benign disorders were mostly paediatric (0–12 years n = 92/159; 12–20 years n = 33/91; 40–60 years n = 4/59; 60+ years n = 2/43).
[c]Patients transplanted for MDS, plasma cell disorders and lymphoma were all adults.

TABLE 2 Final model parameter estimates

Fixed effects: Empirical model			
Parameter	**Estimate**		**95% CI**
V_1 (L/43 kg)	23.4		22–24
Exponent V_1	0.869		0.84–0.88
Clearance at day 1 (L/h/43 kg)	7.58		7.5–7.9
Exponent1 CL: l	1.03		0.95–1.1
Exponent2 CL: p	−0.138		−0.17 to −0.11
V_2 (L/43 kg)	4.83		4–5.8
Q (L/h/43 kg)	5.6		4–8.1
$CL_{decrement}$ after day1 (%)	0.0676		0.05–0.082
Random effects: Empirical model			
Parameter	**Estimate**	**Correlation**	**95% CI**
IIV V_1	13.8%		12–15
IIV CL	19.4%	74.9% (V_1)	18–21
IIV V_2	27.4%		20–36
IOV CL	12.4%		11–13
IOV V_1	12%		10–13
Proportional error (HPLC)	9%		7.8–11
Proportional error (LC–MS)	6.6%		6.4–6.8
Fixed effects: Semi-mechanistic model			
Parameter	**Estimate**		**95% CI**
V_1 (L/43 kg)	23.3		22–24
Exponent V_1	0.863		0.84–0.88
CL at T = 0 (L/h/43 kg)	7.61		7.4–7.8
Exponent1 CL: l	1.04		0.95–1.1
Exponent2 CL: p	−0.14		−0.17 to −0.1
V_2 (L/43 kg)	4.73		3.9–5.7
Q (L/h/43 kg)	5.9		4.1–8.6
S_{GSH} (h/mg, age ≤ 40 years)	0.00259		0.0017–0.0032
Age effect (proportional/year, age > 40 years)	0.0419		0.0062–0.081
Random effects: Semi-mechanistic model			
Parameter	**Estimate**	**Correlation**	**95% CI**
IIV V_1	13.8%		12–15
IIV CL	19.5%	68.4% (V_1)	18–21
IIV V_2	28.6%		20–35
IOV CL	12.1%		11–13
IOV V_1	11.5%		10–13
Proportional error (HPLC)	9.1%		7.7–10
Proportional error (LC–MS)	6.6%		6.4–6.8

2.5 | Nomenclature of targets and ligands

Key protein targets and ligands in this article are hyperlinked to corresponding entries in http://www.guidetopharmacology.org, the common portal for data from the IUPHAR/BPS Guide to PHARMACOLOGY,[33] and are permanently archived in the Concise Guide to PHARMACOLOGY 2019/20.[34]

3 | RESULTS

3.1 | Patient characteristics

A total of 385 patients were included with a median age of 14 years (range 0.16–73), from whom 3994 samples were collected. Of these patients, 292 received busulfan targeted to 90 mg*h/L and 94 received doses targeted to a lower exposure (as described in Section 5.2). Most patients (n = 259) received 160 mg/m^2 fludarabine next to busulfan. Alternative conditioning consisted mostly of either 120 mg/m^2 clofarabine with 40 mg/m^2 fludarabine (n = 68) or 120–200 mg/kg cyclosphosphamide (n = 54) in addition to the targeted busulfan. Serotherapy (rATG) was given to 78% (n = 303) of patients. Detailed patient characteristics are shown in Table 1.

3.2 | Pharmacokinetic models

3.2.1 | Empirical model and exposure

Parameter estimates and 95% CI of the adjusted empirical model (as described in Section 5.3) can be found in Table 2. IIV on clearance, V_1 and V_2 were estimated at 14%, 19%, and 28% respectively. A correlation of 71% between IIV of V_1 and clearance was found. IOV was implemented on V_1 (11%) and clearance (11%). A proportional residual error was separately estimated for samples measured with UV (9.0%) and MS (6.6%). The population mean clearance day 2 onwards was estimated to be 7% (95% CI: 5–8%) lower than day 1. Compared to random IOV, the predicted decrease was limited, illustrated by an estimated difference in clearance between days 1 and 4 ranging from 87% (increase) down to −44% (decrease) as depicted in Figure 2A. In Figure 2B the intra-individual change in clearance from day 1 to day 4 is depicted, stratified for tertiles of individual clearance relative to the population predicted clearance (Equation (2)). The figure suggests that patients with a relatively higher clearance compared to the population value ($CL_{relative}$) have a relatively stronger reduction in clearance compared to patient with a low $CL_{relative}$, who regularly had an increased busulfan clearance over time. No relationship was found between busulfan exposure measures and outcomes (graft versus host disease, graft failure, relapse, nonrelapse mortality and survival). Occurrence of veno-occlusive disease (VOD) or other hepatoxicity events was not reported.

3.2.2 | Semi-mechanistic model

The semi-mechanistic model was developed and final estimates with corresponding SIR-derived 95% CI are shown in Table 2. A similar overall reduction of clearance was estimated compared to the empirical model (Figure 3). However, with the semi-mechanistic model a gradual reduction in clearance was assumed as GSH was presumed to decrease proportional to busulfan metabolism. The S_{GSH} was estimated at 0.0026 h/mg, implying a net relevant GSH reduction of 0.26% per hour for each milligram of busulfan metabolism scaled to 1 L V_1.

Age appeared to have an effect on the time-dependent decline of clearance (Figure 4A), but the effect was only relevant above an age of 40 years (P = 0.009). The effect was modelled as a proportional

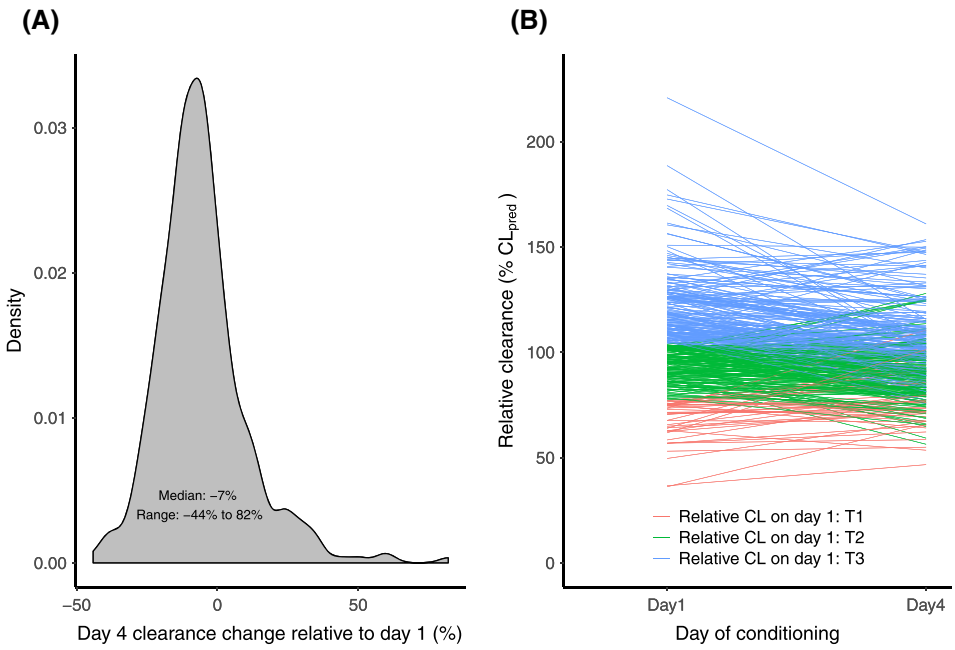

FIGURE 2 Observed variability in busulfan clearance change. (A) A density plot of the relative change of clearance from day 1 to day 4 (%). (B) The change is displayed per individual and stratified in tertiles for relative clearance day 1, defined as the individually estimated clearance divided by the weight-predicted clearance for that individual (%)

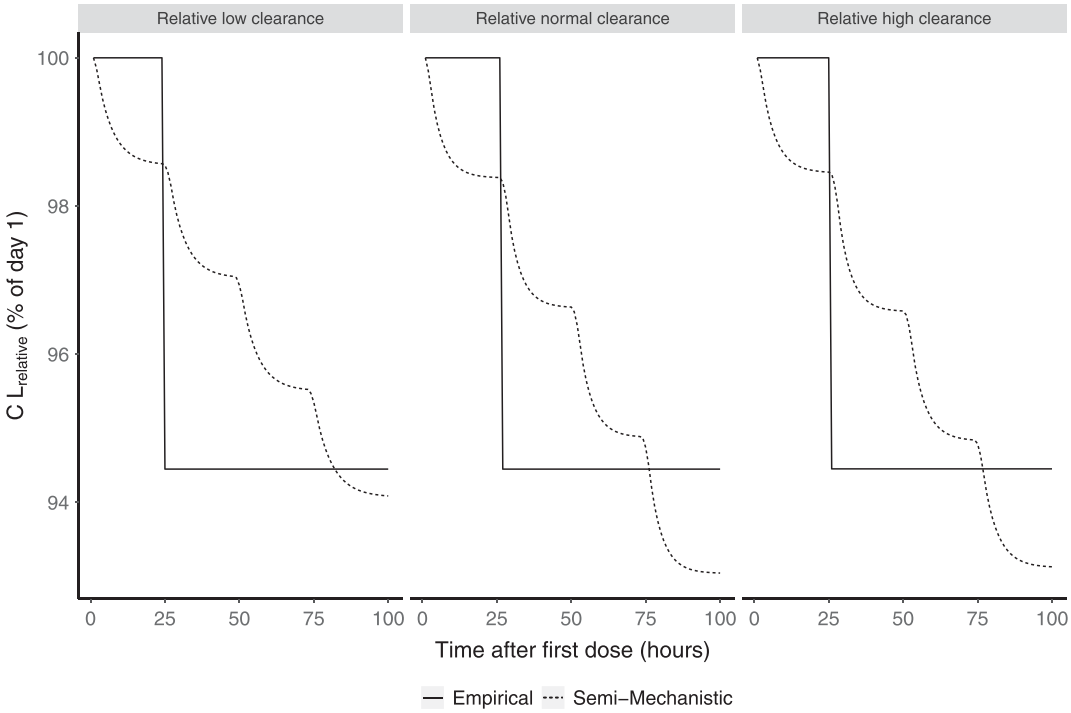

FIGURE 3 Time effect. A display of the time effect for both models. Three individuals were randomly drawn from the each tertile of relative clearance (as defined in Figure 2). The clearance over time is depicted, as predicted per model, based on the day 1 clearance. Values are relative to the day 1 clearance (%)

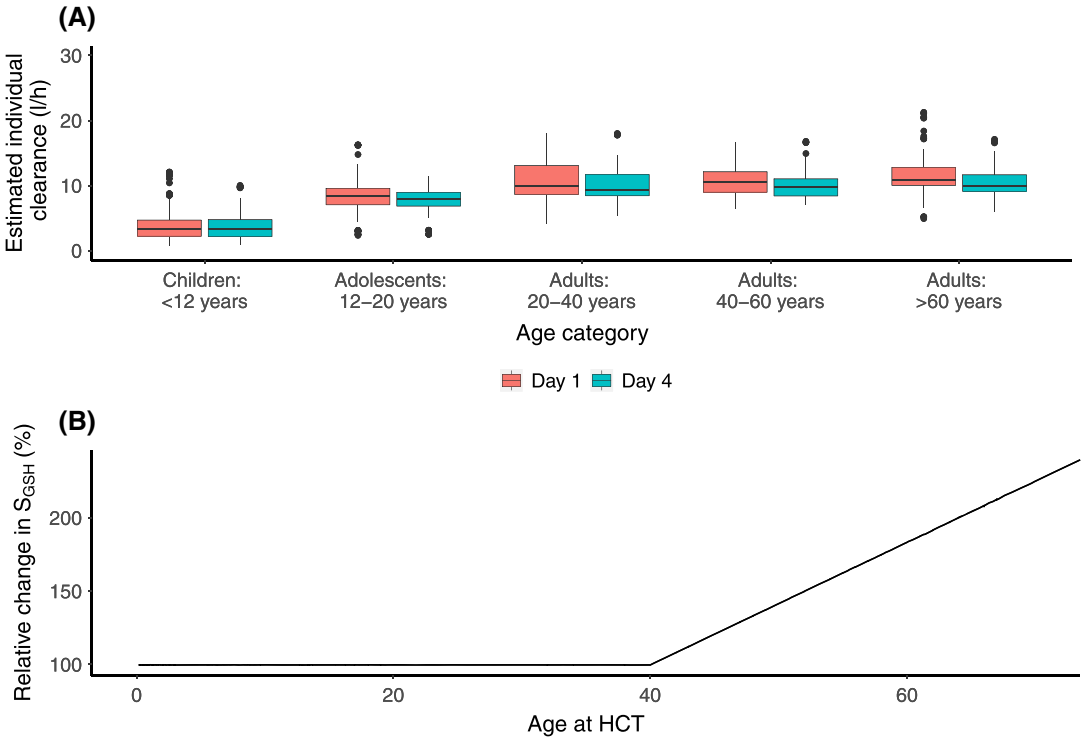

FIGURE 4 Covariate effects. (A) The observed clearance decrements from day 1 to day 4 stratified for age at transplantation. (B) The model predicted decrease of S_{GSH} as implemented in the semi-mechanistic model

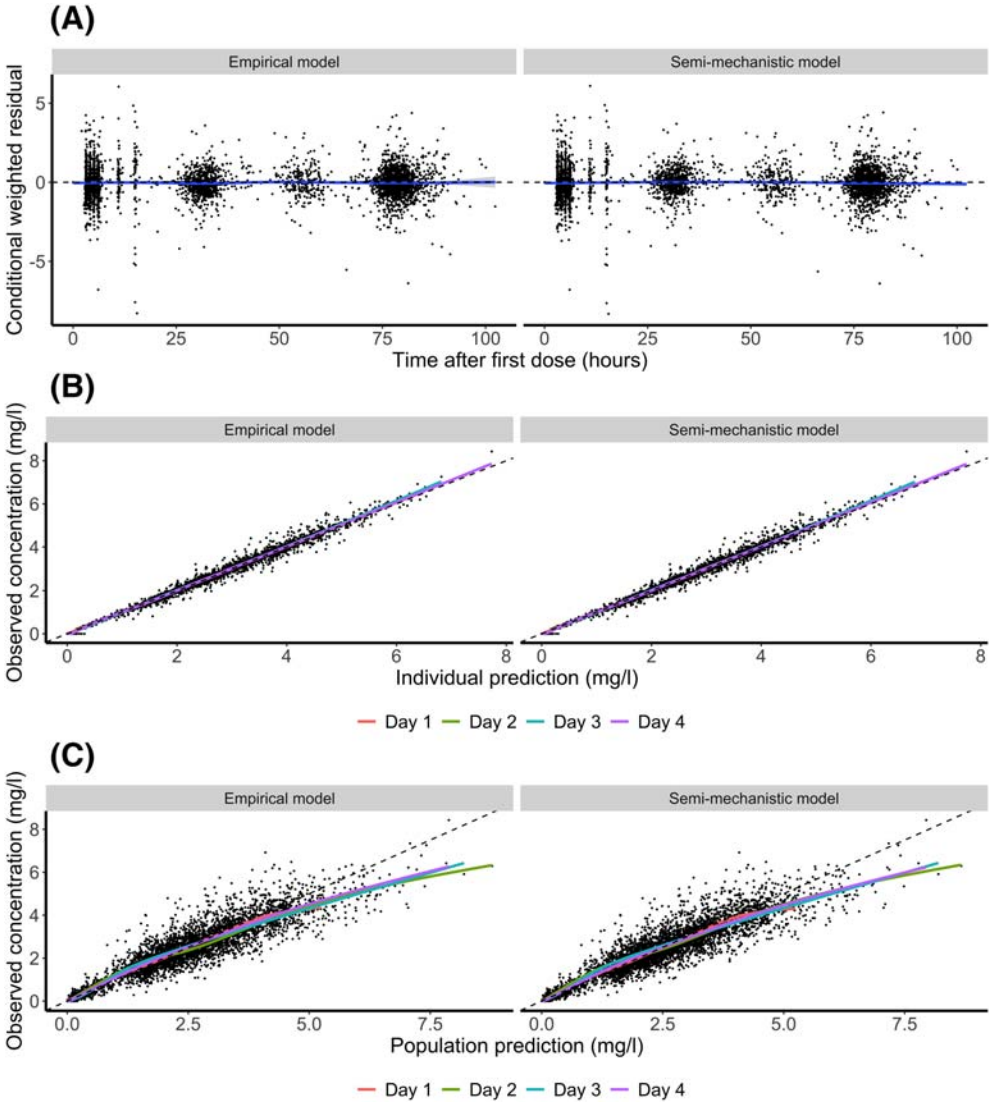

FIGURE 5 Goodness of fit plots. A display of the time effect for both models. Three individuals were randomly drawn from the each tertile of relative clearance (as defined in Figure 2). The clearance over time is depicted, as predicted per model, based on the day 1 clearance. Values are relative to the day 1 clearance (%)

increase of the S_{GSH} of 4% for each year of age (Equation (7)). This resulted in a more than 2-fold increase of the effect from 40 to 73 years of age (Figure 4B).

$$S_{GSH,i} = S_{GSH,pop} \cdot \left(1 + (age_i - 40) \times slope_{Age}\right) \quad (7)$$

Herein, $slope_{age}$ was assumed to be 0 below 40 years of age and was estimated for patients older than 40.

rATG was tested on the time-dependent decline of clearance as a surrogate covariate for paracetamol usage, but no improvement in the model was found.

3.2.3 | Model evaluation

Figure 5 depicts the goodness-of-fit plots for both models. In both models, no time-dependent trends could be observed. In the VPC stratified for days of conditioning no other misspecifications were seen for either model (data not shown).

3.3 | TDM-guided target attainment evaluation

A total of 258 patients were available for TDM simulation, for which the results are reported in Figure 6. Overall, target attainment was slightly better when the semi-mechanistic model was used (top panel, 75%), compared to the empirical model (74%). The final model with age on the S_{GSH} further increased target attainment to 76%. Severe overexposure (>25% above target) was similar for all models, while $AUC_{t0-\infty}$ of >25% below target was not simulated for any of the scenarios. Because of the apparent effect of age, a subset analysis was conducted in children and adults separately. Here it was found that in adults the semi-mechanistic model outperformed the empirical model: 80% *vs* 76% target attainment (Figure 6, bottom panel).

4 | DISCUSSION

To our knowledge, this is the first pharmacokinetic model describing the decrease in busulfan clearance in a large cohort of both children

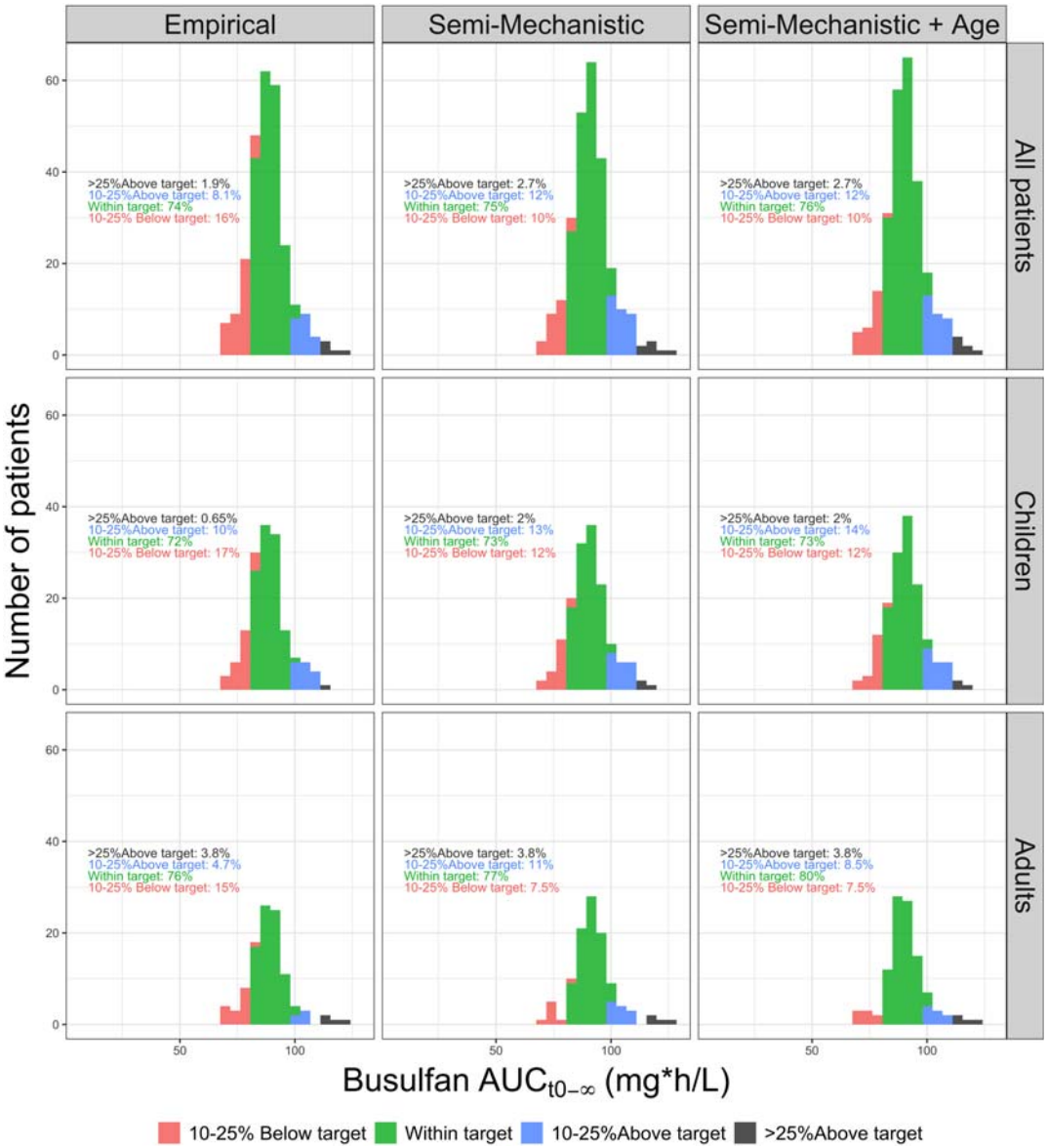

FIGURE 6 Target attainment for different models. Histograms of the simulated busulfan exposure using the empirical model or the semi-mechanistic model with or without age. Results are shown for the full population as well as for children (<20 years) and adults (≥20 years), and the target range is defined as 90 mg*h/L ± 10% (81–99 mg*h/L)

and adult HCT recipients. We demonstrated an overall 7% decline in busulfan clearance over time, which was more pronounced in older adult patients (>40 years of age). The observed clearance reduction of busulfan is of clinical relevance due to a combination of the narrow therapeutic window and a large between-patient variation in clearance over time during the pre-HCT conditioning phase. Furthermore, patients with a high initial busulfan clearance showed a more pronounced decrease compared to patients with a lower initial clearance. For the same dose this would imply that patients with a lower exposure on day 1 (due to a higher clearance) may be overcorrected. Therefore, this metabolism-dependent clearance reduction should be taken into account for precise and accurate targeting of busulfan using TDM. We hypothesized that this reduction in clearance is due to GSH depletion and constructed a semi-mechanistic model, which captured the metabolism-dependent clearance reduction well. Next to biology of GSH homeostasis and GST conjugation, the main arguments in support of the hypothesis are proportionality of the time effect to busulfan metabolism and the increased effect in older age. In TDM simulations, adult patients showed the most improvement in target attainment using the semi-mechanistic model. Underexposure occurred less in these patients, reducing the risk of relapse and graft failure.

In the studied patient cohort, however, no direct relationship between busulfan exposure and outcome was found. TDM was applied for all included patients, causing the range of exposures to be more favourable than in studies were such exposure–outcome relationships were shown.[3–5,7] It is likely, however, that the still somewhat unfavourable exposures observed here would result in

unfavourable outcome probability in a larger population and/or increased nonlethal toxicity.

Besides the direct association between GSH levels and busulfan clearance,[19] there is also indirect evidence from metabolomics. Glycine levels, an important substrate in GSH synthesis, were positively associated with busulfan clearance.[35] Also the age effect is supported by literature and can biologically be explained by older age (60–80 years) being associated with decreased GSH synthesis and thereby absolute levels.[24,25] Here, we found a linear increase in theoretical GSH depletion from the age of 40. Perhaps the latter effect is caused by a relatively low initial GSH reservoir, which results in the same absolute busulfan-dependent depletion of GSH having a more relevant effect on clearance in patients aged 40 years and older. In addition, GST polymorphisms have been linked to busulfan clearance with variable results,[13–18] which can be explained using the presented hypothesis. Though patients with increased GST activity would initially have a higher clearance, they would also have faster GSH depletion. Thus, the average clearance over multiple doses may be similar to patients with less active GST subtypes. In the proposed setting, TDM accounts for the difference in initial clearance and the semi-mechanistic model predicts the concurrent extent of GSH depletion.

Furthermore, the GSH-dependent time effect might have other implications that were not quantified in this study. For example, other drugs that affect busulfan pharmacokinetics or GSH stores such as antifungal agents or paracetamol[36] could interact with the busulfan time effect. In addition, treatment with *N*-acetylcysteine may be helpful in preventing severe side effects during treatment with busulfan. In previous research *N*-acetylcysteine was found to potentially serve as prophylactic agent against sinusoidal obstructive syndrome induced by busulfan.[37,38] Also, evidence was provided that *N*-acetylcysteine does not interfere with the myeloablative effect of busulfan. Thus *N*-acetylcysteine may be suitable to reduce the risk of hepatotoxic side effects of busulfan during conditioning regimens for hematopoietic stem cell transplantation. However, a randomized prospective study assessing *N*-acetylcysteine as a prophylactic agent for VOD did not show any relevant effect[39] as VOD occurrence was rare in both arms suggesting that this trial was underpowered.

A major strength of the current study is the large sample size, with a good distribution of patients over different age groups and limited missing data. As these time-dependent effects are subtle and variable, information including sufficient data over a wide age range was essential for proper quantification of effects. Nevertheless, some weaknesses remain. As direct measurement of GSH was unavailable, busulfan clearance was used as a surrogate. Future studies should focus on measuring active GSH levels before and during the conditioning and implement these in the constructed semi-mechanistic model. The developed mechanistic model can then be expanded with resynthesis of GSH. GSH levels can be measured also in the time course after a busulfan dose has been cleared and before administration of the subsequent dose, where most GSH resynthesis is expected to take place. Preferably, this should be preceded by in vivo (animal) data to support a relationship between plasma and liver levels, as it is known that most GSH is stored in red blood and hepatic cells.[40]

In summary, these data suggest that the intra-individual decrease in busulfan clearance may be related to GSH depletion. This effect increases after an age of 40 years and is proportional to busulfan metabolism. Therefore, busulfan dosing guided by TDM, taking into account the decrease in clearance using the newly constructed semi-mechanistic model, can increase target attainment in patients undergoing conditioning prior to HCT.

ACKNOWLEDGEMENTS

This work was supported by Foundation Children Cancerfree ("Stichting Kinderen Kankervrij", KiKa) project number 190.

COMPETING INTERESTS

J.B., A.C.G.E., A.L., E.vM., J.J.B., C.vK. and A.H. declare to have no conflict of interest. J.K. receives research funding from, and is CSO and shareholder of, Gadeta (www.gadeta.nl). J.L. works at Pharmetheus AB as a consultant for various pharmaceutical companies (www.pharmetheus.com).

CONTRIBUTORS

J.L., J.B., J.J.B., C.vK., A.E., A.L., A.H. and E.vM. designed the study. J.L., J.B. and A.H. analysed the data. J.J.B. and J.K. included patients, provided medical insight and critically appraised the manuscript.

DATA AVAILABILITY STATEMENT

The data that support the findings of this study are available from the corresponding author upon reasonable request.

ORCID

Jurgen B. Langenhorst https://orcid.org/0000-0001-6593-3002

REFERENCES

1. Hahn T, McCarthy PL Jr, Hassebroek A, et al. Significant improvement in survival after allogeneic hematopoietic cell transplantation during a period of significantly increased use, older recipient age, and use of unrelated donors. *J Clin Oncol*. 2013;31(19):2437-2449.
2. Ciurea SO, Andersson BS. Busulfan in hematopoietic stem cell transplantation. *Biol Blood Marrow Transplant*. 2009;15(5):523-536.
3. Andersson BS, Thall PF, Madden T, et al. Busulfan systemic exposure relative to regimen-related toxicity and acute graft-versus-host disease: defining a therapeutic window for i.v. BuCy2 in chronic myelogenous leukemia. *Biol Blood Marrow Transplant*. 2002;8(9):477-485.
4. Bartelink IH, Lalmohamed A, van Reij EM, et al. Association of busulfan exposure with survival and toxicity after haemopoietic cell transplantation in children and young adults: a multicentre, retrospective cohort analysis. *Lancet Haematol*. 2016;3(11):e526-e536.
5. Russell JA, Kangarloo SB, Williamson T, et al. Establishing a target exposure for once-daily intravenous busulfan given with fludarabine and thymoglobulin before allogeneic transplantation. *Biol Blood Marrow Transplant*. 2013;19(9):1381-1386.
6. Palmer J, McCune JS, Perales M-A, et al. Personalizing busulfan-based conditioning: considerations from the American Society for Blood and Marrow Transplantation Practice Guidelines Committee. *Biol Blood Marrow Transplant*. 2016;22(11):1915-1925.
7. Andersson BS, Thall PF, Valdez BC, et al. Fludarabine with pharmacokinetically guided IV busulfan is superior to fixed-dose

delivery in pretransplant conditioning of AML/MDS patients. *Bone Marrow Transplant*. 2017;52(4):580-587.
8. Bartelink IH, Boelens JJ, Bredius RG, et al. Body weight-dependent pharmacokinetics of busulfan in paediatric haematopoietic stem cell transplantation patients: towards individualized dosing. *Clin Pharmacokinet*. 2012;51(5):331-345.
9. Long-Boyle JR, Savic R, Yan S, et al. Population pharmacokinetics of busulfan in pediatric and young adult patients undergoing hematopoietic cell transplant: a model-based dosing algorithm for personalized therapy and implementation into routine clinical use. *Ther Drug Monit*. 2015;37(2):236-245.
10. McCune JS, Bemer MJ, Barrett JS, Scott Baker K, Gamis AS, Holford NH. Busulfan in infant to adult hematopoietic cell transplant recipients: a population pharmacokinetic model for initial and Bayesian dose personalization. *Clin Cancer Res*. 2014;20(3):754-763.
11. BUSULFEX (busulfan) for injection FDA label. https://www.Accessdata.Fda.gov/drugsatfda_docs/label/2015/020954s014lbl.pdf.
12. Myers AL, Kawedia JD, Champlin RE, et al. Clarifying busulfan metabolism and drug interactions to support new therapeutic drug monitoring strategies: a comprehensive review. *Expert Opin Drug Metab Toxicol*. 2017;13(9):901-923.
13. Ansari M, Krajinovic M. Can the pharmacogenetics of GST gene polymorphisms predict the dose of busulfan in pediatric hematopoietic stem cell transplantation? *Pharmacogenomics*. 2009;10(11):1729-1732.
14. Ansari M, Lauzon-Joset JF, Vachon MF, et al. Influence of GST gene polymorphisms on busulfan pharmacokinetics in children. *Bone Marrow Transplant*. 2010;45(2):261-267.
15. Choi B, Kim MG, Han N, et al. Population pharmacokinetics and pharmacodynamics of busulfan with GSTA1 polymorphisms in patients undergoing allogeneic hematopoietic stem cell transplantation. *Pharmacogenomics*. 2015;16(14):1585-1594.
16. Kim SD, Lee JH, Hur EH, et al. Influence of GST gene polymorphisms on the clearance of intravenous busulfan in adult patients undergoing hematopoietic cell transplantation. *Biol Blood Marrow Transplant*. 2011;17(8):1222-1230.
17. Yin J, Xiao Y, Zheng H, Zhang YC. Once-daily i.v. BU-based conditioning regimen before allogeneic hematopoietic SCT: a study of influence of GST gene polymorphisms on BU pharmacokinetics and clinical outcomes in Chinese patients. *Bone Marrow Transplant*. 2015;50:696-705.
18. Zwaveling J, Press RR, Bredius RG, et al. Glutathione S-transferase polymorphisms are not associated with population pharmacokinetic parameters of busulfan in pediatric patients. *Ther Drug Monit*. 2008;30(4):504-510.
19. Almog S, Kurnik D, Shimoni A, et al. Linearity and stability of intravenous busulfan pharmacokinetics and the role of glutathione in busulfan elimination. *Biol Blood Marrow Transplant*. 2011;17(1):117-123.
20. Langman LJ, Danso D, Robert E, Jannetto PJ. High-throughput quantitation of busulfan in plasma using ultrafast solid-phase extraction tandem mass spectrometry (SPE-MS/MS). *Methods Mol Biol*. 2016;1383:89-95.
21. Zwaveling J, Bredius RG, Cremers SC, et al. Intravenous busulfan in children prior to stem cell transplantation: study of pharmacokinetics in association with early clinical outcome and toxicity. *Bone Marrow Transplant*. 2005;35(1):17-23.
22. Cremers S, Schoemaker R, Bredius R, et al. Pharmacokinetics of intravenous busulfan in children prior to stem cell transplantation. *Br J Clin Pharmacol*. 2002;53(4):386-389.
23. Proost JH, Meijer DK. MW/pharm, an integrated software package for drug dosage regimen calculation and therapeutic drug monitoring. *Comput Biol Med*. 1992;22(3):155-163.
24. Rathbun WB, Murray DL. Age-related cysteine uptake as rate-limiting in glutathione synthesis and glutathione half-life in the cultured human lens. *Exp Eye Res*. 1991;53:205-212.
25. Van Lieshout EM, Peters WH. Age and gender dependent levels of glutathione and glutathione S-transferases in human lymphocytes. *Carcinogenesis*. 1998;19(10):1873-1875.
26. Sheiner LB, Rosenberg B, Marathe VV. Estimation of population characteristics of pharmacokinetic parameters from routine clinical data. *J Pharmacokinet Biopharm*. 1977;5(5):445-479.
27. R Core Team. R: a language and environment for statistical computing. R Foundation for Statistical Computing, Vienna, Austria. 2017. URL https://www.R-project.org/.
28. Keizer RJ, van Benten M, Beijnen JH, Schellens JH, Huitema AD. Pirana and Pcluster: a modeling environment and cluster infrastructure for NONMEM. *Comput Methods Programs Biomed*. 2011;101(1):72-79.
29. Hooker AC, Staatz CE, Karlsson MO. Conditional weighted residuals (CWRES): a model diagnostic for the FOCE method. *Pharm Res*. 2007;24(12):2187-2197.
30. EMEA. Guideline on reporting the results of population pharmacokinetic analyses. 2007.
31. FDA. Guidance for industry, population pharmacokinetics. 1999.
32. Bergstrand M, Hooker AC, Wallin JE, Karlsson MO. Prediction-corrected visual predictive checks for diagnosing nonlinear mixed-effects models. *AAPS j*. 2011;13:143-151.
33. Harding SD, Sharman JL, Faccenda E, et al. The IUPHAR/BPS Guide to PHARMACOLOGY in 2018: updates and expansion to encompass the new guide to IMMUNOPHARMACOLOGY. *Nucleic Acids Res*. 2018;46(D1):D1091–D1106. https://doi.org/10.1093/nar/gkx1121
34. Alexander SPH, Kelly E, Mathie A, et al. THE CONCISE GUIDE TO PHARMACOLOGY 2019/20: Introduction and Other Protein Targets. *Br J Pharmacol*. 2019;176(Suppl 1):S1–S20. https://doi.org/10.1111/bph.14747
35. Navarro SL, Randolph TW, Shireman LM, Raftery D, McCune JS. Pharmacometabonomic prediction of busulfan clearance in hematopoetic cell transplant recipients. *J Proteome Res*. 2016;15:2802-2811. 8 Aug.
36. Slattery JT, Wilson JM, Kalhorn TF, Nelson SD. Dose-dependent pharmacokinetics of acetaminophen: evidence of glutathione depletion in humans. *Clin Pharmacol Ther*. 1987;41:413-418.
37. Sjöö F, Aschan J, Barkholt L, Hassan Z, Ringdén O, Hassan M. N-acetyl-L-cysteine does not affect the pharmacokinetics or myelosuppressive effect of busulfan during conditioning prior to allogeneic stem cell transplantation. *Bone Marrow Transplant*. 2003;32(4):349-354.
38. Hassan Z, Hellstrom-Lindberg E, Alsadi S, Edgren M, Hagglund H, Hassan M. The effect of modulation of glutathione cellular content on busulphan-induced cytotoxicity on hematopoietic cells in vitro and in vivo. *Bone Marrow Transplant*. 2002;30(3):141-147.
39. Barkholt L, Remberger M, Hassan Z, et al. A prospective randomized study using N-acetyl-L-cysteine for early liver toxicity after allogeneic hematopoietic stem cell transplantation. *Bone Marrow Transplant*. 2008;41(9):785-790.
40. Halliwell B, Gutteridge JMC. *Free radicals in biology & medicine*. 5th ed. Oxford: Oxford University Press; 2015.

How to cite this article: Langenhorst JB, Boss J, van Kesteren C, et al. A semi-mechanistic model based on glutathione depletion to describe intra-individual reduction in busulfan clearance. *Br J Clin Pharmacol*. 2020;86:1499–1509. https://doi.org/10.1111/bcp.14256